ELSEVIER

Precambrian Research 117 (2002) 157–183

Precambrian Research

www.elsevier.com/locate/precamres

The source and origin of terrigenous sedimentary rocks in the Mesoproterozoic Ui group, southeastern Russia

Robert L. Cullers [a,*], Victor N. Podkovyrov [b]

[a] *Department of Geology, Kansas State University, 108 Thompson Hall, Manhattan, KS 66506-3201, USA*
[b] *Institute of Precambrian Geology and Geochronology RAS, St. Petersburg 199034, Russia*

Received 11 December 2001; accepted 1 April 2002

Abstract

Arenites, wackes, and associated shales and siltstones of the Ui group of Riphcan age in southeastern Siberia have been analyzed for petrographic, major element and selected trace element compositions (including the REE). Petrographic results suggest that the arenites may have been derived from granites and that the wackes may have been derived from more plagioclase-rich rocks like tonalites or granodiorites. The high quartz relative to other materials in many sandstones suggest that they may have been derived from intense chemical weathering or diagenesis so the mineralogic ratios may have been changed during these processes. The shales and siltstones are composed mostly of illite and quartz. In addition, A–CN–K diagrams indicate that the wackes and associated shales and siltstones underwent K-metasomatisim. Extrapolation of the shales and siltstones associated with the wackes back to the plagioclase–alkali feldspar line in the A–CN–K diagram suggests a high average plagioclase to alkali feldspar ratio in the provenance (tonalite to granodiorite). Extrapolation of shales and siltstones associated with the arenites suggest a low plagioclase to alkali feldspar ratio in the provenance (granite). In addition, the index of compositional variability (ICV) and chemical index of alteration (CIA) parameters of the shales and siltstones suggest the weathering of the first cycle material was intense. Trace element ratios suggest all the sedimentary rocks were derived from mostly granitoids. Shales and siltstones were plotted as elemental ratios (e.g. Th/Sc vs. Eu/Eu*). These plots suggest a mix of a granodiorite–tonalite source (for the source of the shales and siltstones associated with the wackes) with a granite source (for the shales and siltstones associated with the arenites). The arenites also contain lower Eu/Eu* and higher Th/Co and Th/Sc ratios than the wackes. This, as is consistent with the petrography, suggests that the arenites were derived from a source with more granite and less granodiorite–tonalite than the wackes.

Keywords: Sandstones; Shales; Provenance; Trace elements; REE; Mesoproterozoic

1. Introduction

The quartz–feldspar–fine-grained lithic fragments (QFL) of sandstones have been used to infer provenance and tectonic environments

* Corresponding author. Fax: +1-913-532-5159
E-mail address: rcullers@ksu.edu (R.L. Cullers).

0301-9268/02/$ - see front matter
PII: S0301-9268(02)00079-7

(Dickinson, 1985; Dickinson and Suczek, 1979; Ingersoll et al., 1984). Major and trace element compositions or ratios and the isotopic composition of sandstones also have been used to further constrain provenance (Bhatia, 1983; Bhatia and Crook, 1986; Cullers, 1994b, 2000; Cullers and Berendsen, 1998; McLennan et al., 1993, 1990; Roser and Korsch, 1986, 1988; Taylor and McLennan, 1991; Van de Kamp and Leake, 1985; Wronkiewicz and Condie, 1990). For example, A–CN–K plots (molar ratios of Al_2O_3–Na_2O + CaO–K_2O) have been used to estimate the alkali feldspar to plagioclase ratios of source rocks and the extent of K-metasomatism of associated shales (Fedo et al., 1995, 1997a,b). Also trace element ratios such as Th/Sc and Eu/Eu* have been used to distinguish sandstones derived from different source rocks and to infer tectonic setting (McLennan et al., 1993).

The mineralogy of shales and siltstones have been of less use than the mineralogy of arkosic sandstones in determining the provenance since many minerals in such rocks formed during weathering and diagenesis. The major element, trace element and isotopic compositions of shales and siltstones, however, have been important in determining provenance and in some cases, tectonic setting (Allègre and Rousseau, 1984; Bavinton and Taylor, 1980; Bhatia, 1985; Condie and Wronkiewicz, 1990; Cox et al., 1995; Cullers, 1994b, 1995, 2000; McLennan et al., 1983; Mongelli et al., 1996). For instance, index of compositional variability's ($ICV = Fe_2Q_3 + K_2O + Na_2O + CaO + MgO + TiO_2/Al_2O_3$) can be used to assess whether or not a given sequence of shales or siltstones represent first cycle sediment or if they were derived from recycling if diagenesis does not alter the amount of K_2O, Na_2O, or CaO (Cox et al., 1995; Cullers and Podkovyrov, 2000). Ratios of trace elements in shales and siltstones that are concentrated in silicic source rocks (La and Th) relative to those that are concentrated in basic rocks (Co, Cr, Ni) may be used to determine the relative amount of silicic to basic rock input from the source. Also the size of the Eu anomaly (Eu/Eu*), the La/Lu ratios, and three component trace element plots (e.g. La–Th–Co) may also be used to determine the provenance of the shales and siltstones as most basic rocks contain no negative Eu anomaly and often contain low La/Lu ratios, while more silicic rocks are more likely to contain a negative Eu anomaly and often have high La/Lu ratios.

In the current study, the provenance of arkosic sandstones and associated shales and siltstones will be compared with those of the wackes and associated shales and siltstones from the Ui group in southeastern Siberia using the above methods. In addition, the amount of primary and recycled material in the terrigenous sedimentary rocks will be estimated. Finally, the provenance and recycling of terrigenous rocks in the Ui group will be compared with a previously studied unit, the Lakhanda group (Cullers and Podkovyrov, 2000) a unit of similar age that was deposited in the same basin.

2. Geology

The area studied is located in southeastern Siberia along the Siberian platform and the Verkhayansk fold belt in the Uchur–Maya region (Fig. 1). Deposition of the platform sedimentary rocks occurred during Riphean to Vendian time (Mesoproterozoic to Neoproterozoic, 1.60–0.54 Ga) with up to 14 km of mostly sediment accumulating over a region of about 600 by 500 km (Khudoley et al., 2001; Semikhatov, 1991; Semikhatov and Serebrykov, 1983; Vinogradov et al., 1998). The sections that are most complete occur in the Gornostakh anticline along the Belaya river and in other parts of the marginal Yudoma–Maya depression (Khudoley et al., 2001). Sections in the Yudoma–Maya platform are thinner than those in the Gornostakh anticline.

Sedimentary rocks of the Riphean age (1.60–0.65 Ga) are composed mostly of terrigenous rocks and marine limestones and dolostones. The rocks of Riphean age are divided into six groups, and are, in ascending order, the Uchur, Aimchan, Kerpyl, Lakhanda, Ui, and Yudoma groups (Table 1; Khudoley et al., 2001; Semikhatov,

1991; Semikhatov and Serebrykov, 1983; Vinogradov et al., 1998). The Lakhanda and Ui groups are of upper Riphean age (Semikhatov, 1991), Geochronological ages for basic sills intruding the lower Kandyk formation (lower Ui) include a Sm–Nd whole rock age of 942 ± 18 Ma (Pavlov et al., 1992) and a U–Pb zircon age of 1005 ± 4 Ma (Rainberd et al., 1998). The more recent study thus suggests that the lower Ui group is older than 1000 Ma.

The Ui group is the focus of this study. It contains more terrigenous rocks than the underlying groups, and it exhibits abrupt changes in thickness and fades (Khudoley et al., 2001). Minor basalts occur in some parts of the Ui group, especially in the central part of the Yudoma–Maya depression. The proportion of rocks in the region of this study is 35–49% arkose–quartz arenite, 20–25% wacke, 26–45% shale–siltstone, and 3% basic igneous rocks. The local names of the sedimentary formations of the Ui group will not be used in the results and discussion sections due to the large lateral variations in lithology and rock associations. Instead, samples within the Ui group will be classified as to whether they were obtained from arkosic sandstones and associated shales and siltstones or whether they were obtained from wackes and associated shales and

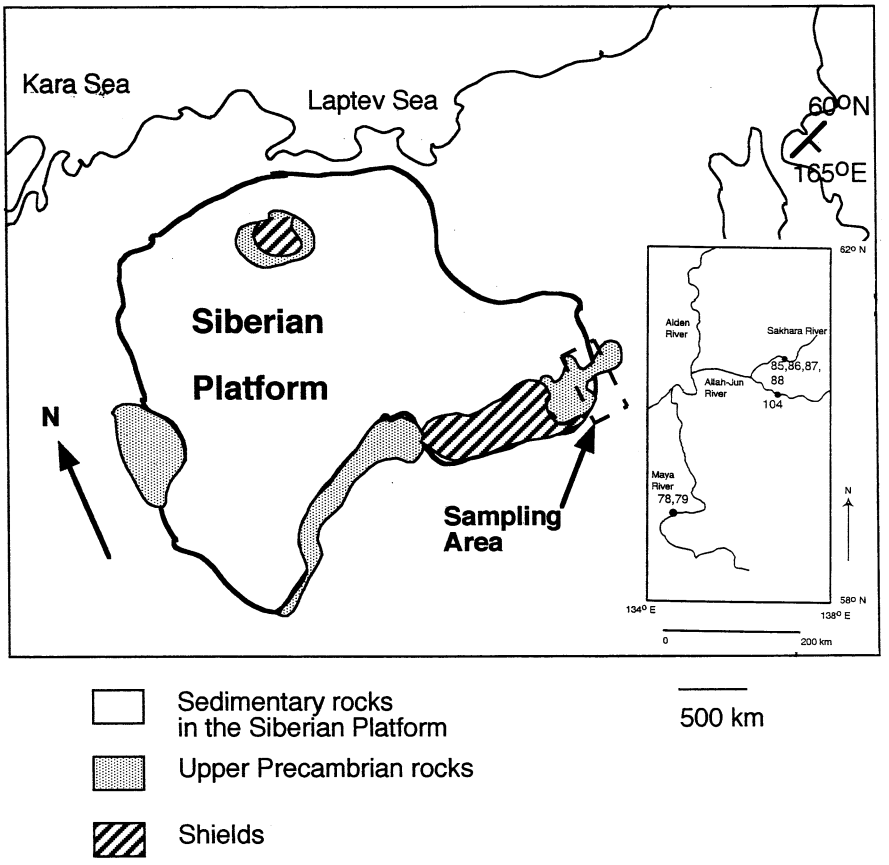

Fig. 1. Index map of the area in which samples were collected along the southeastern edge of the Siberian platform. The heavy dashed rectangle in the map is the area for the inset. Inset is the location of the section from which samples were collected along the Sakhara river (sections 85–88), Allah-Yun river (section 104), and Maya river (sections 78, 79). Within each section, the samples with the lowest numbers (e.g. 85-1) are in the lowest portion of the section and the sample numbers gradually increase upwards to the highest number at the top (e.g. 88-35).

Table 1
Relative stratigraphic sequence of the Riphean rocks in southeastern Siberia

Group	Age	Nature of Sediment
Ui	1000-1030 Ma	arkoses, wackes, shales, siltstones, basalts
Lakhanda		limestones and shales
Kerpyl	1050-1350 Ma	shales, siltstones, quartz and arkosic arenites
Aimchan		dolostones, shales, siltstones, quartz arenites
Uchar	1650-1350 Ma	dolostones, shales, siltstones, quartz and arkosic arenites

siltstones. These divisions appear to reflect best the differences in composition observed within the Ui group.

The names of the sedimentary formations, however, will be mentioned briefly here along with sample locations. The Kandyk formation (section 86 and 87, Sakhara river; section 104, Allakh-Yun river) and the Ryabinovsk formation (section 104, Allakh-Yun river) contain arkoses and associated fine-grained terrigenous rocks (Fig. 1 and Tables 2 and 3). The Kandyk formation (section 78) and Ust-Kirba formation (section 79) are arenites and associated fine-grained terrigenous sedimentary rocks occurring in the Maya platform along the Maya river (Fig. 1 and Tables 2 and 3). The Kandyk formation and Ust-Kirba formation also contain minor basalt in sections transitional to the Yudoma–Maya depressions and up 15–35% by volume in the Ryabinovsk and Malosakhara formations (section 104, Allakh-Yun river) in the central part of the Yudoma–Maya depression. The Malosakhara formation (sections 85 and 88, Sakhara river) and the Dalynda formation (section 104, Allakh-Yun river) mostly contain wackes and associated fine-grained terrigenous sedimentary rocks.

The Kandyk formation in the lower Ui group in the Yudoma–Maya depression along the Sakhara river contains gray–green shales, siltstones, and sandstones up to 1400 m thick (Sukhorukov, 1986). The sandstones range from quartz arenites to subarkose (Khudoley et al., 2001). The main provenance was likely from the Siberian craton to the west or the non-Siberian region to the east (Khudoley et al., 2001). The general rock structure and mineralogic changes within the Kandyk suggests that it reached deep epigenesis (Vinogradov et al., 1998). These epige-

netic alterations likely reset the Rb–Sr and K–Ar ages of the fine-grained terrigenous material to younger ages than the rocks were deposited (Vinogradov et al., 1998).

The middle of the Ui group contains wackes and associated shales, siltstones, and subarkosic sandstones in the Malosakhara and Dalynda formations (Khudoley et al., 2001). The wackes were probably derived mainly from local sources within the basin (Khudoley et al., 2001).

3. Sampling and methods

Forty-nine samples were analyzed for major element and selected trace elements using X-ray fluorescence in the Central Chemical Laboratory, NW Geological Centre, St. Petersburg, Russia, or the IGGD RAS, St. Petersburg along with USGS standard rocks. About 200–400 g of each sample were obtained. One half of each sample was used for thin sections or polished sections for microprobe, and the other half was ground for chemical analysis. The SiO_2 and Al_2O_3 precisions are better than 5% and the precision in FeO (total), TiO_2, MgO, CaO, P_2O_5 MnO, and Na_2O is better than 8%. The precision of trace elements is better than 8%.

The concentration of 39 of the above samples were analyzed for FeO (total), Na_2O, Co, Sc, Hf, Th, Ba, Rb, La, Ce, Nd, Sm Eu, Tb, Yb, and Lu by neutron activation at Kansas State University (Gordon et al., 1968; Jacobs et al., 1977). The precision of most elements was better than 5% although Yb and Lu are better than 7%. The analytical results of standard rocks are periodically analyzed and compared with accepted values (Cullers et al., 1987, 1985).

The mineralogy of the shales and siltstones was determined by semi-quantitative X-ray diffraction. Sandstone petrology was determined using the Gazzi-Dickinson point counting method in which only fine-grained pieces of rock are counted as rock fragments (Ingersoll et al., 1984).

4. Results

4.1. Mineralogy

The shales and siltstones of the Ui group are composed mostly of illite and quartz with lesser amounts of feldspar (plagioclase > alkali feldspar), smectite, and ferromagnesian minerals (magnetite, hematite, chlorite, or ilmenite). For example, shales from the Kandyk formation along the Maya platform (samples 78-27 and 78-29) contain mostly quartz and illite (2M1 > 1Md, including 10–15% of expanded illite-smectite), 3–7% plagioclase, and minor orthoclase, hematite, and rutile. The low to middle Kandyk shales along the Sakhara river also have a similar composition, but the upper Kandyk shales (samples 87-26 and 87-30) contain more plagioclase, Fe–Mg chlorite and traces of rutile and anatase.

Table 2
Correlation of formations within the Ui group

Yudoma–Maya depression			Southeastern portion of the Yudoma–Maya depressions		
Formation	Units present	Section number	Formation	Units present	Section number
Dalynda and Dzhoron	Shales, wackes, minor arenites and basalt	104, Allakh-Yun river	Ust-Kirba	Shales, arenites, minor basalt in eastern sections	79, Maya river
Malosakhara	Shales and wackes	85 and 88, Sakhara river			
Ryabinovsk	Arenites, shales, minor basalt	104, Allakh-Yun river			
Kandyk	Arenites, shales, minor basalt	86 and 87, Sakhara river 104, Allakh-Yun river	Kandyk	Arenites, shales	78, Maya river

Table 3
The chemical composition of Ui sequence rocks (A blank space means that the analysis was not done)

Element	Ui sequence, Sakhara river–Kandyk formation arkoses and associated shales								
	86-3 Sandstone	86-5 Sandstone	86-7 Sandstone	87-1[a] Sandstone	87-3[a] Sandstone	87-4 Sandstone	87-9 Sandstone	87-26 Shale	87-27 Sandstone
SiO_2	98.1	81.09	75.25	66.34	74.53	72.01	92.18	52.90	77.51
TiO_2	0.26	0.40	0.36	0.90	0.01	0.13	0.09	1.53	0.39
Al_2O_3	0.87	8.72	12.01	12.15	0.88	11.89	4.22	21.77	10.81
FeO (total)	0.57	1.55	2.22	5.97	0.55	2.84	0.23	5.91	3.21
Fe_2O_3	0.3	0.47	1.24	2.41	0.27	1.88	0.3	7.08	1.52
FeO	0.3	1.06	1.23	4.12	0.28	1.15	0.3	–	1.36
MnO	0.01	0.02	0.01	0.14	0.11	0.03	0.01	0.05	0.01
MgO	0.18	1.21	1.60	3.35	1.07	4.46	0.32	2.03	1.11
CaO	0.06	0.38	0.38	2.46	13.65	0.30	0.03	0.54	0.27
Na_2O	0.2	2.22	2.49	1.31	0.2	1.03	0.084	1.12	1.47
K_2O	0.05	2.73	3.42	0.98	0.11	3.79	2.24	6.51	3.26
P_2O_5	0.05	0.19	0.14	0.12	0.05	0.09	0.05	0.20	0.09
LOI	0.3	1.04	1.86	3.17	8.44	2.70	0.54	6.13	2.07
Total	100.61	99.55	99.74	96.89	99.60	99.27	99.99	98.69	100.20
Rb	6	69	89	37	5	152	84	289	151
Ba	377	670	660	205	391	534	388	803	695
Sr	1.6	51	83	110	310	46	27	59	40
Th	1.5	9.6	14.8	6.0		12.3	2.8	23.3	9.1
Zr	40	350	290	250	69	480	300	400	280
Hf		9.1	7.8	6.9		11.4	8.2	10.3	7.9
Nb	<1	34	12	8.1	<1	12	<1	26	7.9
Ta		0.78	1.3	0.77		1.1	0.24	2.1	0.87
Co		3.4	2.0	19.0		5.8	0.30	11.1	6.2
Sc		6.1	4.9	17.9		8.1	0.79	22.0	7.0
Cr		32	22	57.9		40	9.4	121	28
Cs		0.46	0.63	0.99		4.4	1.2	12.2	2.5
La		38.5	79.2	21.6		37.9	16.4	74.4	26.1
Ce		81.8	155	49.3		74.4	33.4	148	51.7
Nd		38.9	65.6	21.1		33.9	15.7	61.9	24.7
Sm		7.70	12.5	4.24		7.08	3.41	12.3	5.08
Eu		1.28	1.61	1.10		1.12	0.49	1.93	0.91
Tb		0.95	1.25	0.65		0.89	0.35	1.27	0.64
Yb		3.19	3.78	2.52		3.37	1.11	5.66	2.45
Lu		0.48	0.57	0.38		0.52	0.18	0.85	0.34
Eu/Eu[a]		0.554	0.458	0.806		0.533	0.496	0.567	0.600
(La/Lu)cn		8.01	13.9	5.6		7.3	8.84	8.73	7.54
La/Sc		6.3	16.2	1.2		4.7	20.8	3.4	3.7
Th/Sc		1.6	3.0	0.34		1.5	3.5	1.1	1.3
La/Co		11.3	39.6	1.1		6.5	54.7	6.7	4.2
Th/Co		2.8	7.4	0.32		2.1	9.3	2.1	1.5
La/Cr		1.2	3.6	0.37		0.95	1.7	0.61	0.93
Th/Cr		0.30	0.67	0.10		0.31	0.30	0.19	0.33
CIW′-I	0.726	0.705	0.746	0.849	0.728	0.875	0.968	0.922	0.817
ICV	1.95	1.37	1.21	1.79	32.42	1.67	0.88	0.65[b]	1.11
CIA	0.639	0.544	0.586	0.612	0.034	0.652	0.617	0.72[b]	0.627

Table 3 (*Continued*)

Element	Ui Sequence, Sakhara river–Malosakhora formation wackes and associated shales									
	87-28[a] Sandstone	87-30 Shale	88-31 Shale	88-33[a] Sandstone	88-35[a] Sandstone	85-3 Sandstone	85-5 Siltstone	85-20 Shale	85-21 Sandstone	85-24 Siltstone
SiO_2	72.79	57.79	60.88	77.99	78.51	72.28	63.99	62.28	75.68	61.07
TiO_2	0.41	0.99	0.96	0.51	0.51	1.27	1.18	0.77	0.85	1.41
Al_2O_3	9.06	18.32	17.93	8.35	7.33	9.83	15.73	18.65	11.72	15.93
FeO(total)	4.32	7.88	5.95	4.04	3.97	6.40	7.08	5.52	3.21	8.84
Fe_2O_3	1.53	9.53	2.69	1.73	1.82					
FeO	3.31	–	3.53	2.64	2.67					
MnO	0.13	0.09	0.06	0.08	0.09	0.17	0.09	0.03	0.03	0.10
MgO	1.43	2.89	2.19	1.97	1.86	1.97	2.54	1.71	0.55	2.73
CaO	3.22	0.36	0.72	0.98	1.71	2.16	0.96	0.76	1.29	0.92
Na_2O	2.07	2.01	1.52	1.99	1.63	2.39	1.61	1.80	2.22	1.68
K_2O	2.03	4.37	4.98	1.28	0.95	1.16	3.74	4.83	3.00	3.90
P_2O_5	0.11	0.15	0.16	0.28	0.31	0.08	0.14	0.12	0.04	0.15
LOI	3.66	3.74	4.25	1.84	2.49	2.00	2.10	3.12	1.25	2.70
Total	99.23	98.59	99.60	99.31	99.36	99.71	99.16	99.59	99.84	99.43
Rb	68	183	200	47	40	34	133	206	119	140
Ba	411	597	713	221	225	224	525	617	760	426
Sr	110	83	88	45	44	57	86	98	132	90
Th	7.2	14.1		6.1	5.3	5.4	7.3	13.3	19.8	9.5
Zr	300	290	330	260	350					
Hf	7.3	7.5		7.9	8.7	7.7	6.4	6.5	17.5	5.3
Nb	6.5	21	18	6.3	6.6					
Ta	0.66	1.5		0.57	0.53	0.60	0.75	1.3	1.3	1.1
Co	7.4	14.8		9.9	12.8	11.9	15.8	19.6	7.5	29.9
Sc	5.5	15.4		8.1	7.5	9.9	12.6	15.2	6.6	13.9
Cr	23	68		35	33	31	40	61	39	56
Cs	1.0	6.3		0.96	1.0					
La	25.2	61.7		29.3	23.2	21.5	16.5	37.0	51.3	23.8
Ce	48.3	121		57.3	46.1	40.0	34.3	67.8	93.8	56.4
Nd	20.1	52		22	18.6	18.8	21.7	33.9	42.2	29.0
Sm	3.91	10.6		4.52	3.44	3.79	5.85	7.44	7.87	6.90
Eu	0.96	1.71		0.94	0.73	0.76	1.33	1.40	1.42	1.34
Tb	0.62	1.21		0.63	0.50	0.50	0.90	1.03	0.97	0.90
Yb	2.44	4.01		2.46	2.08	2.2	2.82	3.8	4.43	2.76
Lu	0.38	0.62		0.37	0.33	0.33	0.43	0.57	0.69	0.41
Eu/Eu[a]	0.763	0.564		0.656	0.667	0.66	0.711	0.613	0.606	0.647
(La/Lu)cn	6.6	10.0		7.82	7.04					
La/Sc	4.6	4.0		3.6	3.1	2.2	1.3	2.4	7.8	1.7
Th/Sc	1.3	0.92		0.75	0.71	0.55	0.58	0.88	3.00	0.68
La/Co	3.4	4.2		3.0	1.8	1.8	1.0	1.9	6.8	0.8
Th/Co	1.0	1.0		0.62	0.41	0.45	0.46	0.68	2.64	0.32
La/Cr	1.1	0.91		0.84	0.70	0.69	0.41	0.61	1.32	0.43
Th/Cr	0.31	0.21		0.17	0.16	0.17	0.18	0.22	0.51	0.17
CIW′-1	0.727	0.847	0.878	0.718	0.732	0.714	0.856	0.863	0.762	0.852
ICV		1.00[b]	0.83[b]				1.11[b]	0.73[b]	0.92[b]	1.23[b]
CIA		0.76[b]	0.82[b]				0.82[b]	0.82[b]	0.69[b]	0.81[b]

Table 3 (*Continued*)

Element	Ui Sequence, Allakh-Yun river Kandyk formation Ryabinovsk formation arkoses and associated shales						
	85-25 Sandstone	85-34 Shale	85-35 Sandstone	104-1[a] Sandstone	104-5 Sandstone	104-10[a] Sandstone	104-12 Shale
SiO_2	64.17	50.74	65.52	70.62	95.90	68.47	52.48
TiO_2	0.88	1.58	1.34	0.90	0.11	0.43	1.08
Al_2O_3	15.31	20.01	12.95	11.43	1.62	9.76	20.46
FeO(total)	6.95	9.09	7.25	3.21	0.60	4.00	8.31
Fe_2O_3				1.14	0.3	1.37	3.61
FeO				2.31	0.33	2.98	5.86
MnO	0.13	0.09	0.09	0.07	0.01	0.18	0.08
MgO	2.87	3.60	2.69	1.47	0.21	1.32	2.78
CaO	1.18	1.49	1.43	2.96	0.22	5.86	0.86
Na_2O	3.03	1.06	2.81	2.87	0.2	2.83	2.67
K_2O	2.92	5.91	2.76	2.83	0.11	0.60	4.51
P_2O_5	0.07	0.20	0.15	0.34	0.47	0.27	0.34
LOI	2.30	5.71	2.00	3.66	0.37	5.37	4.95
Total	99.81	99.48	98.99	100.36	99.82	99.09	98.52
Rb	102	266	90	115	8	43	221
Ba	408	684	309	484	384	93	641
Sr	118	62	124	150	2.9	110	32
Th	7.7	18.2	7.7	24.2		8.4	19.2
Zr				990	360	210	210
Hf	5.8	6.2	6.2	26.0		6.2	5.4
Nb				20	2	9.3	23
Ta	0.88	1.8	0.87	1.7		1.2	1.8
Co	15.8	18.1	17.5	3.6		12.0	13.8
Sc	13.0	30.8	12.6	10.3		5.4	23.9
Cr	49	116	52	40		29	121
Cs				3.1		2.2	8.0
La	22.2	43.1	23.7	80.6		19.6	53.3
Ce	45.5	87.4	50.5	145		40.3	107
Nd	22.5	41.2	24.3	56.0		17.3	44.9
Sm	4.81	8.97	5.30	8.83		4.09	8.33
Eu	1.01	1.97	1.12	1.86		0.68	1.41
Tb	0.69	1.39	0.75	1.27		0.76	1.23
Yb	2.56	5.1	2.64	5.90		2.65	4.93
Lu	0.40	0.73	0.39	0.91		0.41	0.73
Eu/Eu[a]	0.667	0.676	0.681	0.658		0.500	0.535
(La/Lu)cn				8.8	4.82	7.34	
La/Sc	1.7	1.4	1.9	7.8		3.6	2.2
Th/Sc	0.59	0.59	0.61	2.3		1.6	0.80
La/Co	1.4	2.4	1.4	22.4		1.6	3.9
Th/Co	0.49	1.01	0.44	6.7		0.70	1.4
La/Cr	0.45	0.37	0.46	2.0		0.68	0.44
Th/Cr	0.16	0.16	0.15	0.61		0.29	0.16
CIW′-1	0.754	0.920	0.737	0.708	0.831	0.677	0.823
ICV	1.35[b]	1.11[b]	1.63[b]		1.21		1.01[b]
CIA	0.62[b]	0.81[b]	0.59[b]		0.656		0.70[b]

Table 3 (*Continued*)

Element	Ui Sequence, Allakh-Yun river Ryabinovsk formation arkoses and associated shales						Dalynda formation wackes and associated shales	
	104-17 Shale	104-20 Shale	104-30 Sandstone	104-34[a] Sandstone	104-40 Sandstone	104-41 Siltstone	104-54 Sandstone	104-56 Sandstone
SiO_2	59.79	60.58	87.65	70.62	90.22	63.34	77.64	77.48
TiO_2	1.07	1.12	0.17	0.28	0.40	0.92	0.44	0.46
Al_2O_3	15.95	16.53	4.41	7.00	4.74	16.5	9.45	9.47
FeO (total)	10.0	8.06	2.02	5.01	1.09	5.87	3.52	3.17
Fe_2O_3	5.65	3.74	0.27	1.80	0.27	1.97	1.44	1.39
FeO	4.46	4.69	1.52	3.63	0.74	3.97	2.21	2.15
MnO	0.05	0.04	0.04	0.12	0.01	0.04	0.03	0.04
MgO	2.02	2.36	0.91	2.35	0.81	2.19	1.89	1.66
CaO	0.09	0.07	1.27	6.36	0.24	0.61	0.47	0.48
Na_2O	2.14	1.94	0.25	0.54	0.045	1.77	2.81	3.22
K_2O	3.02	3.52	0.67	1.09	1.32	4.69	0.85	1.04
P_2O_5	0.42	0.47	0.18	0.33	0.26	0.41	0.44	0.45
LOI	4.95	4.36	1.96	5.45	1.16	3.68	1.77	2.13
Total	99.50	99.05	99.53	99.15	100.30	100.02	99.31	99.60
Rb	151	130	30	44	48	198	33	46
Ba	360	543	147	191	204	630	180	218
Sr	53	42	18	110	2.5	24	40	40
Th	16.2		3.8	5.4	6.9	15.4	8.0	7.3
Zr	230	200	140	98	1320	290	280	250
Hf	6.5		3.3	2.6	35.0	8.0	7.9	8.2
Nb	16	19	5.2	3.2	9.1	16	8.2	6.5
Ta	1.6		0.33	0.48	0.70	1.6	0.73	0.74
Co	39.7		5.0	11.5	3.3	18.6	9.8	9.4
Sc	17.6		3.7	6.6	3.4	16.2	7.5	7.7
Cr	96		21	29	34	76	117	33
Cs	7.4		0.56	0.98	1.3	4.3	0.65	1.1
La	41.5		13.1	20.9	8.4	52.4	36.9	22.4
Ce	88.3		27.0	39.2	18.4	101	69.3	45.1
Nd	58.0		11.8	16.7	7.9	42.9	28.8	19.9
Sm	7.15		2.39	3.31	1.96	8.31	5.29	3.94
Eu	1.32		0.45	0.80	0.33	1.44	0.95	0.92
Tb	1.03		0.33	0.52	0.28	0.83	0.63	0.63
Yb	4.62		1.23	1.72	3.34	3.92	2.54	2.59
Lu	0.70		0.19	0.26	0.59	0.60	0.38	0.40
Eu/Eu[a]	0.586		0.591	0.733	0.529	0.638	0.621	0.706
(La/Lu)cn	5.89		6.80	8.20	1.43	8.75	9.9	5.6
La/Sc	2.4		3.5	3.2	2.5	3.2	4.9	2.9
Th/Sc	0.92		1.0	0.82	2.0	1.0	1.1	0.9
La/Co	1.0		2.6	1.8	2.5	2.8	3.8	2.4
Th/Co	0.41		0.76	0.47	2.09	0.83	0.82	0.78
La/Cr	0.43		0.62	0.72	0.25	0.69	0.32	0.68
Th/Cr	0.17		0.18	0.19	0.20	0.20	0.07	0.22
CIW′-1	0.819	0.838	0.915	0.887	0.985	0.850	0672	0.641
ICV	1.08[b]	1.22	1.69		1.11	0.91[b]	1.41[b]	1.40[b]
CIA	0.75[b]	0.699	0.561		0.710	0.66[b]	0.61[b]	0.58[b]

Table 3 (*Continued*)

Element	Ui Sequence, Allakh-Yun river Dalynda formation wackes and associated shales				Ui Formation–Maya.platform Kandyk formation arkoses and associated shales				
	104-57 Siltstone	104-59 Sandstone	104-60 Siltstone	104-68 Sandstone	78-21 Shale	78-27 Shale	78-29 Shale	78-32[a] Sandstone	78-40[a] Sandstone
SiO_2	62.42	81.88	61.00	68.47	65.86	67.00	66.35	95.02	92.44
TiO_2	1.01	0.26	1.05	0.58	0.93	0.93	0.95	0.03	0.04
Al_2O_3	16.85	8.32	16.41	13.16	16.85	16.42	17.19	0.52	0.43
FeO(total)	6.08	1.98	7.17	6.90	3.65	3.48	3.53	2.30	0.57
Fe_2O_3	2.27	0.98	2.63	1.64	3.07	3.00	2.95		
FeO	4.23	1.20	4.47	5.52	1.14	0.84	0.96		
MnO	0.05	0.02	0.04	0.09	0.01	0.01	0.01	0.02	0.08
MgO	2.17	0.78	2.75	2.15	1.23	1.21	1.41	0.32	0.65
CaO	0.16	0.23	0.34	0.58	0.28	0.28	0.25	0.58	1.64
Na_2O	1.51	2.91	1.51	2.37	1.11	1.11	1.00	0.01	0.14
K_2O	4.47	1.19	4.77	2.15	4.02	4.53	4.65	0.20	0.05
P_2O_5	0.47	0.48	0.60	0.26	0.05	0.05	0.05	0.04	0.06
LOI	4.17	1.38	4.43	3.07	4.60	4.40	4.68	0.25	0.25
Total	99.36	99.43	100.07	99.78	98.59	99.42	100.07	99.29	96.35
Rb	206	50	211	94		178	221		20
Ba	443	278	557	284		519	441		53
Sr	23	31	23	38					
Th	16.0	5.9	15.9	10.0		14.9	18.6		1.4
Zr	260	280	270	280					
Hf	6.5	6.6	7.5	7.5		9.5	8.6		4.0
Nb	18	4.1	16	9.5					
Ta	1.6	0.47	1.6	0.99		1.4	1.8		0.15
Co	12.3	4.2	19.7	14.0		9.8	11.5		0.51
Sc	19.0	3.0	20.8	11.4		13.4	16.2		0.44
Cr	87	19	82	47		63	83		5
Cs	6.6	2.0	5.7	3.7		8.1	11.0		0.5
La	37.2	34.4	34.3	22.4		39.7	51.7		5.3
Ce	76.5	67.3	72.2	49.1		76.7	91.4		9.3
Nd	30.7	26.6	30.3	21.8		28.6	37.5		3.6
Sm	5.97	5.15	6.33	4.50		5.76	6.95		0.72
Eu	1.14	1.13	1.08	0.98		0.88	1.01		0.14
Tb	0.84	0.59	0.85	0.53		0.75	0.79		0.11
Yb	4.04	1.99	4.24	2.76		3.60	3.89		0.61
Lu	0.58	0.32	0.63	0.43		0.54	0.60		0.11
Eu/Eu*	0.605	0.779	0.550	0.732		0.506	0.509		0.588
(La/Lu)cn	6.37	10.9	5.46	5.24		7.4	8.6		5.06
La/Sc	2.0	11.5	1.6	2.0		3.0	3.2		12.0
Th/Sc	0.84	2.0	0.76	0.88		1.11	1.15		3.18
La/Co	3.0	8.2	1.7	1.6		4.1	4.5		10.4
Th/Co	1.3	1.4	0.81	0.71		1.5	1.6		2.7
La/Cr	0.43	1.8	0.42	0.48		0.63	0.62		1.06
Th/Cr	0.18	0.31	0.19	0.21		0.24	0.22		0.28
CIW′-1	0.872	0.635	0.869	0.771		0.900	0.913		0.651
ICV	0.83[b]	1.08[b]	1.01[b]	1.23[b]	0.80	0.85	0.84		
CIA	0.85[b]	0.58[b]	0.83[b]	0.65[b]	0.716	0.694	0.707		

Table 3 (*Continued*)

Element	Ui formation–Maya platform Ust-Kirba formation arkoses and associated shales				
	79-8 Sandstone	79-9 Shale	79-11 Shale	79-13 Sandstone	79-15 Sandstone
SiO_2	95.26	65.5	63.91	67.72	63.22
TiO_2	0.12	1.00	1.05	0.48	1.17
Al_2O_3	1.20	17.7	17.00	11.13	17.86
FeO (total)	1.66	4.38	4.48	10.47	5.05
Fe_2O_3					
FeO					
MnO	0.01	0.03	0.02	0.24	0.08
MgO	0.10	1.80	2.32	2.28	2.21
CaO	0.16	0.11	0.38	0.42	0.45
Na_2O	0.05	1.27	1.35	1.08	0.95
K_2O	0.45	4.30	4.04	2.69	4.71
P_2O_5	0.02	0.05	0.03	0.03	0.10
LOI	0.25	4.50	4.90	4.40	4.50
Total	99.28	100.64	99.48	100.94	100.12
Rb		220	220	103	
Ba		460	472	433	
Sr					
Th		18.4	17.0	7.6	
Hf		10.0	8.8	8.6	
Ta		1.7	1.6	0.63	
Co		11.9	8.3	10.8	
Sc		16.1	15.8	7.5	
Cr		152	160	30	
Cs		9.9	9.0	2.4	
La		50.3	44.0	27.7	
Ce		83.5	75.3	65.9	
Nd		29.9	29.3	38.3	
Sm		5.89	5.92	9.30	
Eu		1.00	1.00	1.46	
Tb		0.89	0.84	0.91	
Yb		4.22	4.05	3.26	
Lu		0.66	0.62	0.53	
Eu/Eu*		0.533	0.531	0.588	
(La/Lu)cn		7.63	7.09	5.23	
La/Sc		3.1	2.8	3.7	
Th/Sc		1.14	1.08	1.01	
La/Co		4.2	5.3	2.6	
Th/Co		1.5	2.0	0.7	
La/Cr		0.33	0.28	0.92	
Th/Cr		0.12	0.11	0.25	
CIW′-1		0.894	0.884	0.862	
ICV	2.04	0.90	1.00	1.83	1.03
CIA	0.582	0.718	0.700	0.671	0.703

[a] Contains significant calcite.
[b] Corrected for K-metasomatism.

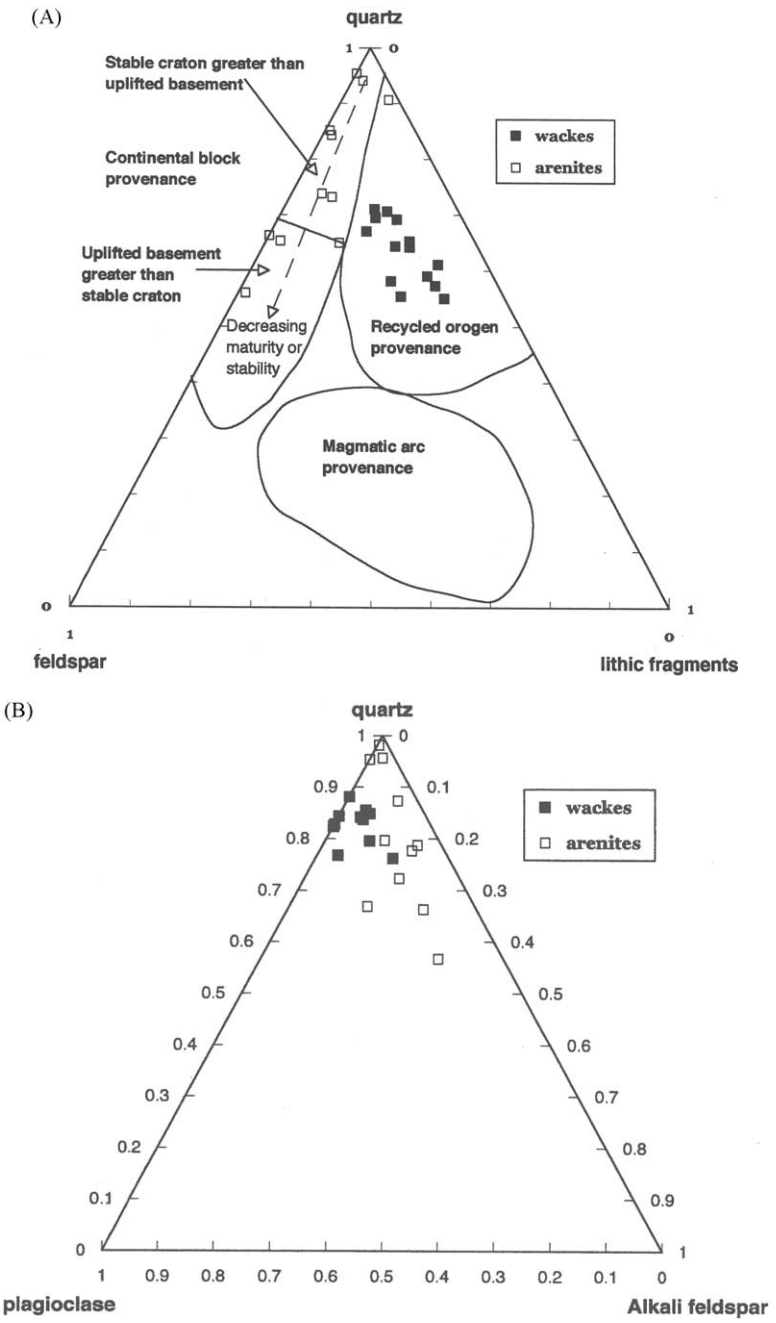

Fig. 2. (a) The relative amount of quartz, feldspar, and rock fragments of representative samples of the wackes and arenites in the Ui group are given. (b) The relative amount of quartz, plagioclase, and alkali feldspar of representative samples of the wackes and arenites in the Ui group are given.

The shales of the Upper Ui group in the Yudoma–Maya sections contain mineralogy that is more variable. The shales of the Malosakhara formation along the Sakhara river (88-13, 85-20,88-31) contain mostly quartz and illite (1 Md illite with 5–20% expanded illite–smectite layers),

10–20% plagioclase (Ab 8–20), less than 5% alkali feldspar, 5–10% magnetite–hematite, 5% Mg–chlorite, and traces of rutile. The shales of the Ryabinovsk formation (104-17, 104-20) along the Allakh-Yun rivers are also mostly illite and quartz with lesser chlorite, smectite, plagioclase, magnetite, and ilmenite. Thus, the shales and siltstones have been diagenetically altered, but no minerals occur that suggests that they have been metamorphosed. The above and other characteristic features of these shales suggest secondary alteration at a temperature of less than 200 °C with low fluid/rock ratios (Pokrovsky and Vinogradov, 2001).

Wackes and arenites contain abundant quartz relative to feldspar and lithic fragments (Fig. 2). This suggests that the sandstones were weathered or diagenetically altered to remove feldspar and lithic fragments and increase the relative amount of quartz relative to the source rock (Nesbitt et al., 1996).

Sandstones from the lower and part of the upper Ui group (Kandyk, Ryabinovsk, and Ust-Kirba formations) are mainly quartz arenites to arkosic arenites. They are composed of mostly very fine to fine, angular to rounded grains. Quartz is quite abundant relative to feldspar and lithic fragments (Fig. 2a). They consist of 47–91% quartz (mostly monocrystalline, non-undulatory with lesser undulatory), 2–39% feldspar and minor rock fragments (mostly shale and siltstone), muscovite–illite, chlorite, biotite, and magnetite–hematite. Alkali feldspars are similar to or greater in amounts than the plagioclase (Fig. 2b). The cement is quartz and/or calcite. The quartz-rich arenites plot in the stable craton environment, whereas, the more feldspar-rich arenites plot in the uplifted basement (Fig. 2a). These relationships imply that the former are more extensively weathered, perhaps as a result of multiple phases of recycling, or have undergone more diagenetic change than the latter. Plots of arenites in quartz–plagioclase–alkali feldspar space (Fig. 2b) suggests derivation of many arenites from steady state weathering of granites such as happened in the Appalachians (Nesbitt et al., 1996).

In contrast, sandstones from the middle and part of the upper Ui group (Maiosakhara and Dalynda formations) are wackes with shale to siltstone fragments more abundant than in the arenites (Fig. 2a). They are composed of mostly very fine to medium, angular to rounded grains. They are composed of 27–54% quartz (mostly monocrystalline, non-undulatory with lesser undulatory quartz), 5–13% feldspar, 2–29% rock fragments, 9–50% clay matrix, and lesser amounts of muscovite, chlorite, magnetite–hematite. The wackes are thus quartz-rich, and they contain plagioclase greater than alkali feldspar (Fig. 2b). They have silica and/or calcite cement. The wackes plot in the recycled orogen provenance in a QFL diagram (Fig. 2a). Abundant lithic fragments in the wackes are, however, mostly shale to siltstone (again mostly composed of illite and quartz). The wackes do contain a minor component of altered basaltic and gabbroic rock fragments. In short, the compositions of the wackes are not similar to those of arc-derived, volcaniclastic sandstones. The abundant quartz and the greater plagioclase relative to alkali feldspar suggest that the wackes could have been derived from plagioclase-rich source rocks such as tonalite and granodiorite (Nesbitt et al., 1996). The abundant shales and siltstones in the wackes suggest that a significant amount of the source could have been recycled. Other investigators have obtained similar results from formations analyzed during this study as well as from other formations within the Ui group (Khudoley et al., 2001).

4.2. Geochemistry

The elemental concentrations and certain elemental ratios of the terrigenous rocks of the Ui group are given in Table 3, and the averages (with one standard deviation) of the arenites, wackes, and the shales and siltstones arc given in Table 4. The wacke and arenite compositions are also compared in Fig. 3a, and the shales and siltstones associated with the wackes and arenites are compared in Fig. 3b in both cases from highest with lowest ratios.

In general, the SiO_2 concentrations and the Eu/Eu*, La/Sc, Th/Sc, and La/Cr ratios are higher in all the sandstones than in all the shales and siltstones (Table 4). In contrast, the TiO_2, Al_2O_3, FeO (total), MgO, and K_2O concentrations of the

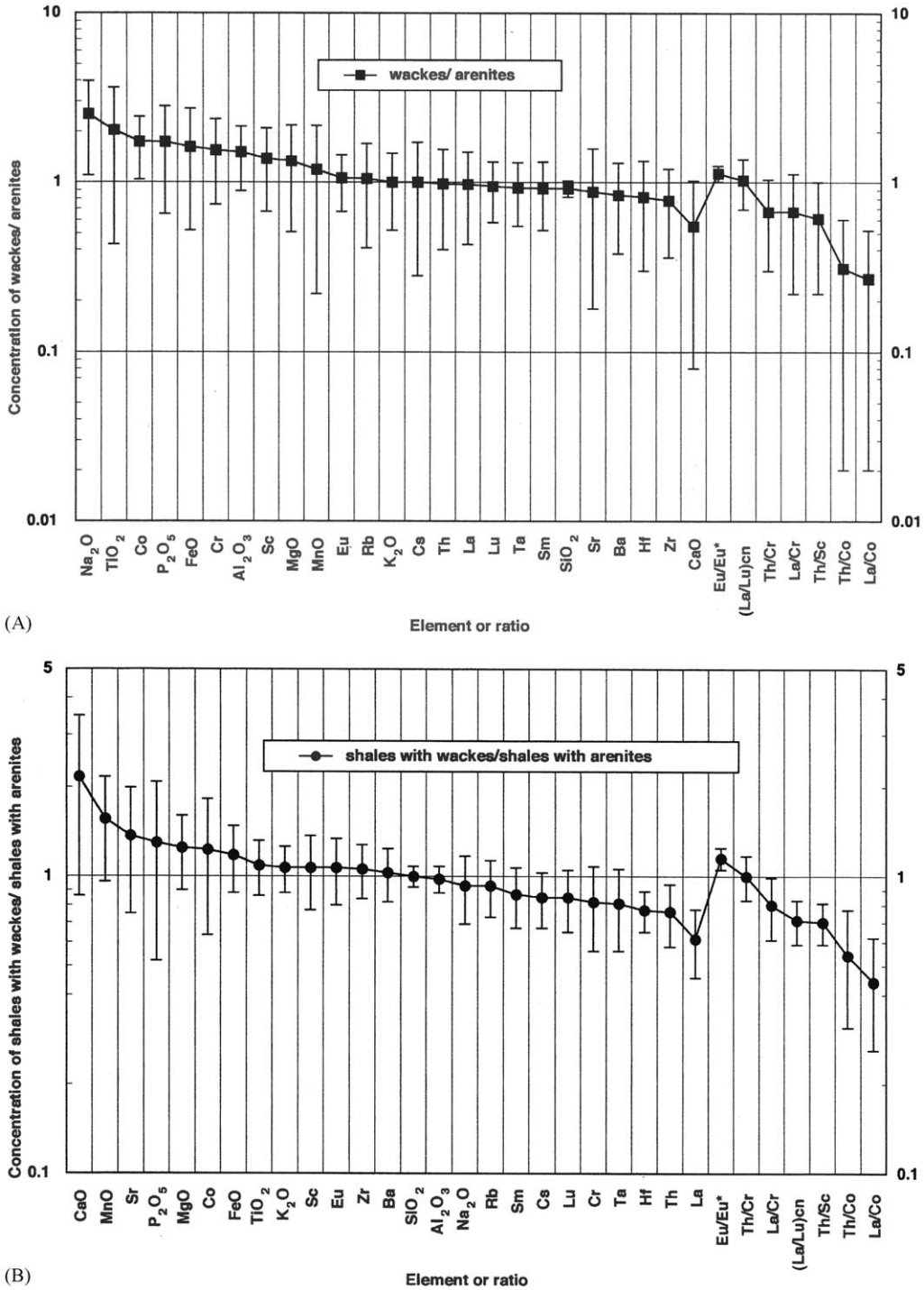

Fig. 3. (a) The log of the elemental composition and ratios of selected elements of the wackes and arenites are compared. (b) The log of the elemental composition and ratios of selected elements associated with the shales and siltstones of the wackes are compared with those associated with the arenites.

sandstones are lower than those of the shales. The higher SiO_2 concentrations and lower Al_2O_3 and K_2O concentrations in the sandstones than the shales and siltstones are probably due to the higher quartz and lower illite–muscovite in the sandstones relative to the shales and siltstones. The lower TiO_2, FeO (total), and MgO concentrations in the sandstones than in the shales and

Table 4
Comparison of the elemental concentrations and ratios of the Ui formation samples with those of the Lakhanda formation (maximum number of samples in parentheses)

Element	Ui group				Lakhanda group [a]	
	Shales associated with arenites(21)	Wacke shales (7)	Arenites (19)	Wackes (10)	Belaya shales (13)	Maya shales (12)
SiO_2	60.7 ± 5.5	60.3 ± 4.0	82.0 ± 11	74.0 ± 6.0	58.9 ± 4.4	53.1 ± 6.5
TiO_2	1.06 ± 0.19	1.14 ± 0.28	0.31 ± 0.27	0.71 ± 0.36	1.253 ± 0.095	1.54 ± 0.19
Al_2O_3	17.8 ± 2.0	17.4 ± 1.6	6.5 ± 4.5	10.6 ± 2.6	21.1 ± 1.7	23.7 ± 2.4
FeO (total)	6.3 ± 2.4	7.1 ± 1.4	2.4 ± 1.7	4.7 ± 1.9	7.27 ± 4.09	8.29 ± 8.0
MnO	0.042 ± 0.03	0.061 ± 0.03	0.06 ± 0.05	0.08 ± 0.05	0.015 ± 0.017	0.035 ± 0.047
MgO	2.01 ± 0.63	2.53 ± 0.60	1.34 ± 1.1	1.84 ± 0.73	1.57 ± 0.49	0.76 ± 0.28
CaO	0.37 ± 0.26	0.76 ± 0.44	2.3 ± 3.5	1.1 ± 0.6	0.40 ± 0.28	0.28 ± 0.09
Na_2O	1.65 ± 0.59	1.53 ± 0.23	1.04 ± 1.03	2.5 ± 0.5	0.55 ± 0.35	0.18 ± 0.15
K_2O	4.4 ± 1.0	4.7 ± 0.7	1.5 ± 1.3	1.7 ± 0.9	4.1 ± 1.3	3.2 ± 1.0
P_2O_5	0.24 ± 0.17	0.26 ± 0.19	0.17 ± 0.13	0.26 ± 0.17	0.081 ± 0.038	0.053 ± 0.023
LOI	4.6 ± 0.7	3.8 ± 1.2	2.6 ± 2.3	2.0 ± 0.5	4.23 ± 0.71	8.54 ± 1.65
Rb	209 ± 39	195 ± 46	63 ± 47	66 ± 32	175 ± 42	140 ± 33
Ba	567 ± 135	544 ± 106	372 ± 200	311 ± 171	396 ± 106	284 ± 89
Sr	49 ± 21	67 ± 32	76 ± 83	67 ± 41	63 ± 39	89 ± 43
Th	17.6 ± 2.8	13.4 ± 4.2	8.5 ± 5.7	8.3 ± 4.3	22.8 ± 5.1	21.1 ± 2.9
Zr	270 ± 75	287 ± 38	365 ± 347	283 ± 35	261 ± 53	288 ± 65
Hf	8.3 ± 1.6	6.4 ± 0.7	10.3 ± 9.0	8.4 ± 3.3	8.6 ± 2.2	8.4 ± 1.8
Ta	1.68 ± 0.20	1.36 ± 0.39	0.83 ± 0.41	0.77(0.25)	2.1 ± 0.4	2.0 ± 0.3
Co	15.5 ± 10	19 ± 6	6.5 ± 5.2	11.3 ± 4.0	15.7 ± 10	15.2 ± 9.3
Sc	17.4 ± 3.4	18.7 ± 6.7	6.3 ± 4.3	8.7 ± 3.0	23.1 ± 5.8	23.4 ± 1.8
Cr	104 ± 36	74 ± 27	29 ± 13	45 ± 27	109 ± 31	102 ± 14
Cs	8.5 ± 2.4	7.2 ± 0.8	1.6 ± 1.2	1.6 ± 1.1		
La	52 ± 11	32 ± 10	30 ± 23	29 ± 10	60.6 ± 15	55.3 ± 9.3
Sm	7.9 ± 2.3	6.9 ± 1.2	5.3 ± 3.3	4.9 ± 1.2	9.4 ± 4.0	8.3 ± 1.8
Eu	1.30 ± 0.36	1.38 ± 0.32	0.94 ± 0.50	1.0 ± 0.2	1.54 ± 0.73	1.51 ± 0.37
Lu	0.66 ± 0.09	0.56 ± 0.12	0.42 ± 0.21	0.40 ± 0.11	0.78 ± 0.22	0.84 ± 0.19
Eu/Eu*	0.55 ± 0.04	0.63 ± 0.06	0.60 ± 0.10	0.68 ± 0.05	0.531 ± 0.094	0.575 ± 0.048
(La/Lu)cn	7.9 ± 1.2	5.6 ± 1.0	7.0 ± 2.8	7.2 ± 1.9	8.0 ± 1.1	6.8 ± 1.1
La/Sc	3.0 ± 0.5	1.7 ± 0.4	6.7 ± 5.7	4.2 ± 3.2	2.66 ± 0.44	2.36 ± 0.31
Th/Sc	1.02 ± 0.12	0.72 ± 0.13	1.79 ± 0.9	1.1 ± 0.79	1.0 ± 0.2	0.90 ± 0.10
La/Co	4.1 ± 1.6	1.8 ± 0.8	11.8 ± 16	3.2 ± 2.4	5.30 ± 3.1	5.60 ± 4.36
Th/Co	1.4 ± 0.5	0.76 ± 0.36	2.8 ± 2.9	0.88 ± 0.69	2.0 ± 1.3	2.1 ± 1.6
La/Cr	0.55 ± 0.20	0.44 ± 0.08	1.15 ± 0.85	0.77 ± 0.46	0.57 ± 0.13	0.54 ± 0.07
Th/Cr	0.18 ± 0.04	0.18 ± 0.02	0.31 ± 0.16	0.21 ± 0.12	0.21 ± 0.03	0.21 ± 0.03
CIA	0.686 ± 0.024	0.660 ± 0.014	0.620 ± 0.048	0.575 ± 0.037	0.78 ± 0.07	0.85 ± 0.03
ICV	1.07 ± 0.2	1.25 ± 0.16	1.41 ± 0.44	1.62 ± 0.32	0.81 ± 0.21	0.62 ± 0.30
K_2O/Al_2O_3	0.27 ± 0.04	0.29 ± 0.02	0.24 ± 0.14	0.17 ± 0.06	0.22 ± 0.04	0.15 ± 0.05

All values are means and 1 S.D.
[a] From Cullers and Podkovyrov (2000).

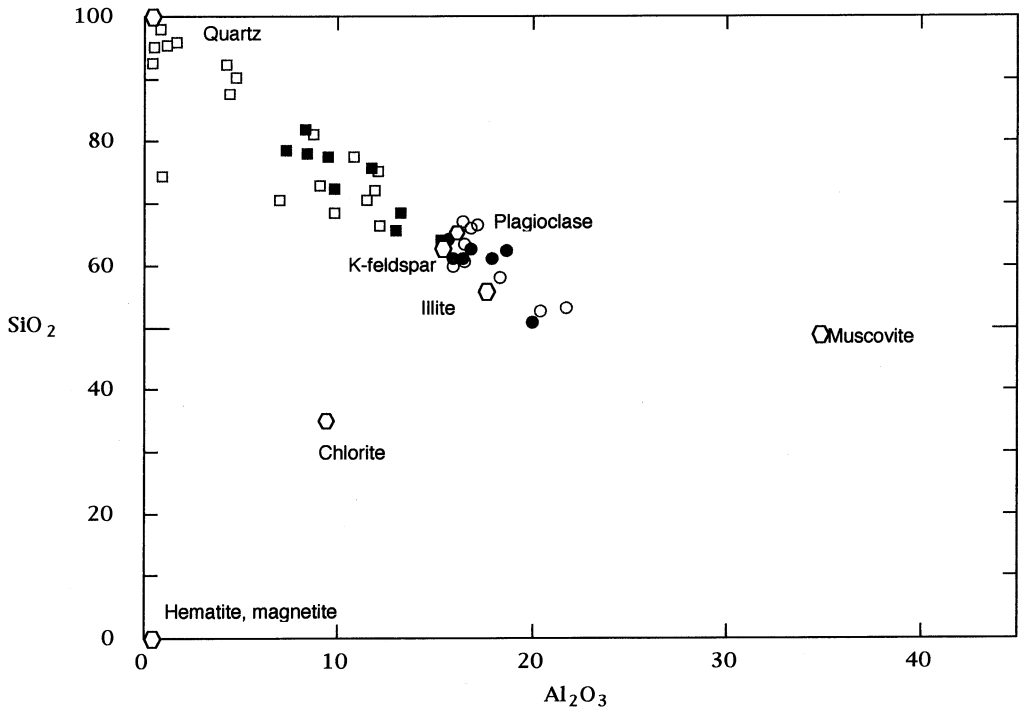

Fig. 4. The SiO_2 and $A1_2O_3$ concentrations of the arenites (open square), shales and siltstones associated with the arenites (open circle), wackes (solid square), and shales and siltstones associated with the wackes (solid circle) are compared with possible mineral composition making up these rocks. The mineral compositions were obtained from microprobe analyses of the minerals in selected samples.

siltstones may be due to the higher chlorite and hematite–magnetite in the shales and siltstones relative to the sandstones.

The SiO_2 concentrations in the wackes are lower than those of the arenites. This result is likely due to the abundant quartz and lower fine-grained content in the arenites relative to the wackes (Fig. 3). The TiO_3, Al_2O_3, FeO (total), Na_2O, Co and Eu/Eu* values are higher in the wackes than in the arenites. This relationship may partially be due to dilution by quartz in the arenites relative to the wackes, to the higher clay mineral content in the wackes relative to the arenites, or to source rock composition. For example, an inverse correlation of SiO_2 and Al_2O_3 is illustrated in Fig. 4. Quartz arenites plot at the highest SiO_2 and lowest Al_2O_3 concentrations due to abundant quartz and absence of most other minerals. The SiO_2 and Al_2O_3 concentrations of the arkosic arenites overlap those of the wackes at lower SiO_2 and higher Al_2O_3 values. This relationship is most likely due to the high Al_2O_3 content of the feldspars in the wackes and arenites and to the high Al_2O_3 content in the clay minerals in the abundant ground mass and sedimentary rock fragments in the wackes. Shales and siltstones contain the highest Al_2O_3 and lowest SiO_2 concentrations presumably due to their higher illite, muscovite, and chlorite, and to their lower amounts of quartz compared with the sandstones. Differences in the trace elements due to possible source rock differences will be given in the discussion section.

The REE plots of the shale–siltstone and sandstone data are given in Fig. 5, and the average concentrations are given in Table 4. Note the wider range of concentrations in the REE of the arenites relative to the wackes and the higher Eu/Eu* in the wackes than in the arenites. On average, however, there is no overall difference of the REE concentrations in the arenites and wackes (Fig. 5 and Table 4). Other elemental concentrations and ratios not mentioned above

are also similar in concentration of the wackes and arenites (Fig. 3a and Table 4).

The La, Ce, Hf, and Th concentrations and the (La/Lu)cn La/Sc, Th/Sc, La/Co, La/Cr, and Th/Co ratios of the shales and siltstones associated with the wackes are lower than those compared with the shales and siltstones associated with the arenites (Table 4 and Fig. 3b). Also the Eu/Eu* of the shales and siltstones associated with the wackes are higher than in the shales and siltstones associated with the arenites. All other major element and trace element concentrations are very similar in the shales and siltstones associated with the wackes and arenites (Fig. 3b). The REE concentrations of the shales and siltstones are plotted in Fig. 5. Note the generally lower (La/Lu)cn ratios and La concentrations, and higher Eu/Eu* of the shales and siltstones associated with the wackes relative to those associated with the arenites. The relation of these values to provenance will be commented on in the discussion section. In addition, the high concentrations of Th, La, Ce, and Hf in the shales and siltstones associated with the arenites relative to those associated with the wackes could be due to differences in the amount of certain accessory minerals like zircon or monazite. For example, a plot of Th/Sc versus Zr/Sc ratios (figure not shown) suggests that some of the variation in the Zr/Sc value may be due to variation in the amount of zircon rather than due to change in provenance. Thus, in some cases, higher Th/Sc ratios in the upper Kandyk quartz arenites may indicate marked input of recycled material (McLennan et al., 1993). The lack of correlation of Zr or Hf to Ti or heavy REE, however, does not support the idea that the accessory minerals are a major control on the composition of these elements.

5. Discussion

5.1. A–CN–K diagrams—implications for diagenesis and provenance

The molar ratios of Al_2O_3–$(CaO^* + Na_2O)$–K_2O may be plotted in triangular A–CN–K diagram to distinguish chemical weathering, K-metasomatism, and source rock compositions (Fedo et al., 1995, 1997a,b). The CaO included in the carbonate minerals and apatite can be subtracted from the total CaO content before plot-

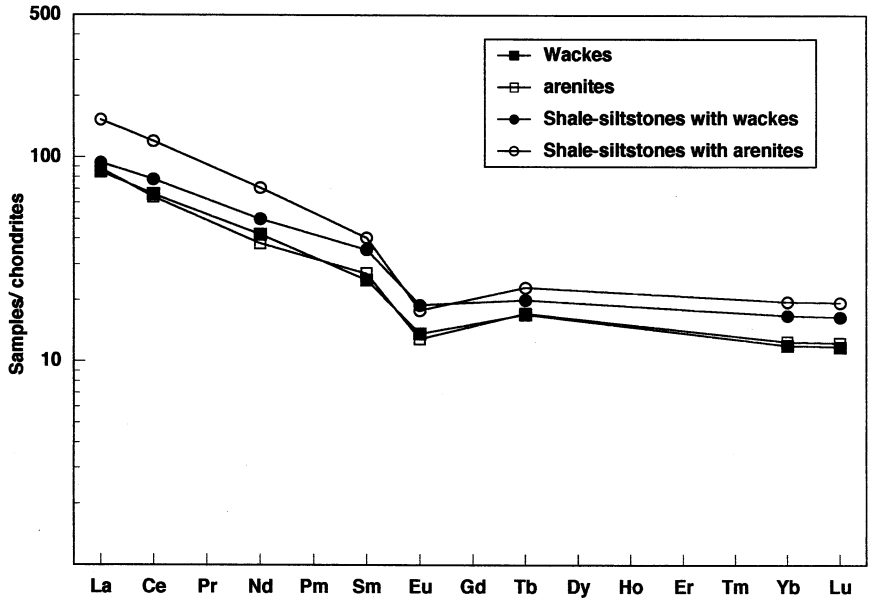

Fig. 5. The average REE content of the wackes, arenites, and the shales and siltstones associated with wackes and arenites are normalized to chondrites (Nakamura, 1974). This graph does not emphasize the wide range in concentration of the arenites.

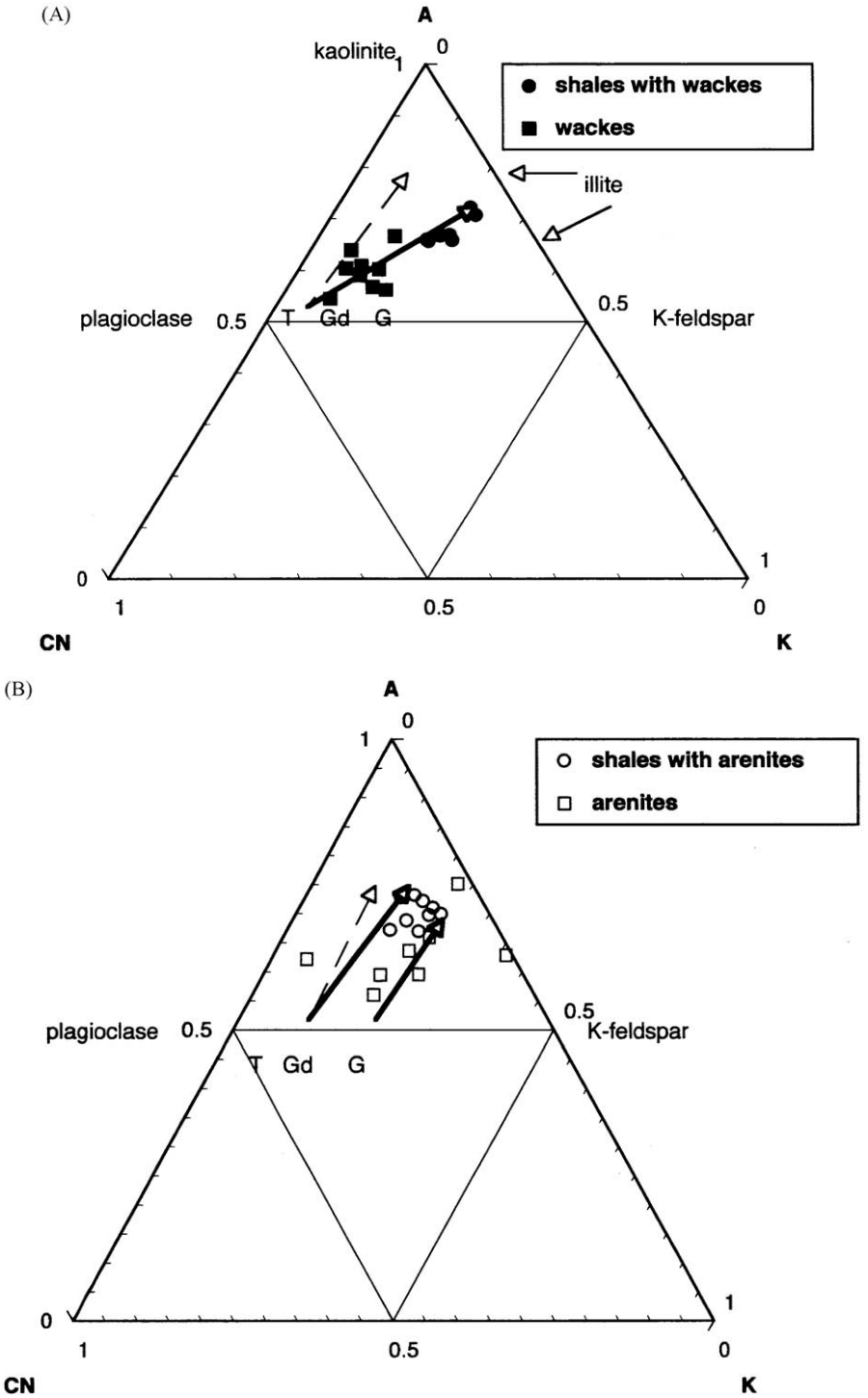

Fig. 6. (a) (top) The A–CN–K plot of the wackes and associated shales and siltstones suggest variation due to K-metasomatism (solid line) that extends back to a tonalite to granodiorite source. The dashed line parallel to the A–CN face could be variation due to weathering only. (b) (bottom). The A–CN–K plot of the arenites and associated shales and siltstones shows a lot of scatter. There could be some variation due to K-metasomatism (solid lines) back to granodiorite or even tonalite composition or to weathering (dashed line) back to granite composition.

ting the molar ratios to give the CaO*. Here we subtracted the CaO in apatite assuming all the P_2O_5 was present in apatite. Samples with carbonate minerals were not plotted since CO_2 in the rocks was not determined.

Clay minerals formed from plagioclase–alkali feldspar rocks as predicted from kinetic leach rates should plot along lines parallel to the CN side of A–CN–K diagram (Fig. 6a, dashed line; Fedo et al., 1995, 1997a,b). For example, tonalite should plot on the plagioclase side of the feldspar join so clay minerals formed from the rock should plot along the dashed line if no other process affects the samples. Thus, clay-rich shales and siltstones may be extrapolated back to the plagioclase–alkali feldspar line to suggest the plagioclase/alkali feldspar ratio in the original rock. The K-metasomatism of weathered rocks originally containing kaolinite can produce illite resulting in a trend at right angles to the A–K join (solid line, Fig. 6a). The average alkali feldspar to plagioclase ratio of the source after K-metasomatisni may still be estimated (bottom left of the solid line, Figure 6a).

Sandstones may have two extreme paths of K metasomatism (Fedo et al., 1995), In one path, the Al-rich minerals like kaolinite may be converted to illite so that the samples change to K-rich compositions much like that described for the shales. In the second process, plagioclase may be converted to authegenic alkali feldspar to move the composition of the sandstone to more K-rich composition.

In our samples, alkali feldspar has not petrographically replaced plagioclase, but illite has replaced feldspar and thus perhaps the original kaolinite in the feldspar. Thus, the sandstones may have had some K-enrichment just like the shales and siltstones. Also the wackes contain abundant illite in the matrix and shale–siltstone fragments so they may have had K-enrichment The wackes and associated shales produce data that lie along a fairly tight cluster at right angles to the A–K join (Fig. 6a), suggesting that the samples were affected by metasomatism, A regression line through the points can be extended back to the plagioclase–alkali feldspar join (solid line). The intersection suggests a high plagioclase to alkali feldspar ratio in the source such as a basalt, tonalite, or granodiorite.

The shales and siltstones associated with the arenites plot in a fairly tight cluster so that a regression line cannot be fit with much confidence (Fig. 6b). The ranges of regression lines in an A–CN–K diagram (solid lines) appear to project back to the feldspar join at a higher amount of alkali feldspar to plagioclase than for the shales associated with the wackes.

The above results are consistent with the modes of the arkoses and wackes. The high amount of quartz relative to feldspar and lithic rock fragments in the wackes and arenites suggests that they may have had significant chemical weathering of a granitoid source or diagenetic alteration to form the sandstones. In addition, the arenites contain more alkali feldspar relative to plagioclase than do the wackes. Thus, the modal results, like the A–CN–K diagrams suggest that the arenites could have been derived from granites and the wackes could have been derived from tonalites or granodiorites. Most notably the wackes were not likely derived from any significant amount of basalts.

5.2. CIA's-relation to weathering intensity

Also the chemical index of alteration (CIA) of the rocks may be read directly off the vertical axis of the A–CN–K diagram (Fedo et al., 1995; Nesbitt and Young, 1982). For example, unweathered rocks have CIA's of about 50, and an unmetasomatised shale plotting at the upper end of the dashed line would have a CIA of about 80 (Fig. 6a). The K-metasomatism also lowers the CIA of the samples. The original CIA of the samples may be reconstructed back to the sample compositions prior to metasomatism (solid line back to the dashed line parallel to the A–K boundary Fig. 6a; Fedo et al., 1995).

The present CIA of the shales and siltstones associated with the wackes ranges from 67 to 73. The CIA's extended back to the composition prior to metasomatism ranges from about 81 to 85. This suggests that intense weathering produced these shales and siltstones.

5.3. ICV-relation to recycling and weathering intensity

The Index of Compositional Variability (ICV $= Fe_2O_3 + K_2O + Na_2O + CaO + MgO + TiO_2 +$

Al_2O_3) may be used to assess the original composition of shales and siltstones (Cox et al., 1995). The non-clay minerals in the original rocks have higher values of ICV's than do the clay minerals. The ICV's of constituent minerals increase, for instance, in the order kaolinite ($\sim$0.03–0.05), montmorillionite ($\sim$0.15–0.3), muscovite–illite ($\sim$0.3), plagioclase ($\sim$0.6), alkali feldspar ($\sim$0.8–1), biotite ($\sim$8), and amphibole–pyroxene ($\sim$10–100; Cox et al., 1995). Therefore, in relatively unaltered shales and siltstones composed mostly of feldspar, pyroxene, amphibole, or biotite with less abundant clay minerals ICV's should tend to be greater than one. Such shales and siltstones are usually deposited as first cycle deposits in technically active areas (Pettijohn et al., 1987; Van de Kamp and Leake, 1985). Shales and siltstones with abundant clay minerals tend to have ICV's less than one and form in areas of minimal uplift and are associated with extensive chemical weathering (Cox et al., 1995). Sands deposited in such areas approach a quartz arenite in composition. First cycle terrigenous sediment formed during intense chemical weathering or with long residence times in soils, however, may also become intensely weathered (Barshad, 1966; Johnsson, 1988, 1993, 2000) and thus form ICV's less than one. Thus, shales and siltstones with ICV's greater than one are most likely first cycle sediments, and those with ICV's less than one may be recycled or intensely weathered first cycle sediment.

The ICV's of the wackes, shales, and siltstones of the Ui group have been calculated using corrected K_2O values obtained from the CIA's in the A–CN–K diagrams (Tables 1 and 2). The ICV's of the arkosic and quartz arenites have been calculated from the original data. The variation in K_2O before and after metasomatism, however, produces very little change in the ICV value. Samples with carbonate minerals have been excluded from this tabulation. Many of the shales and siltstones have ICV's that average close to one, but ranges from 0.65 to 1.23 (Tables 1 and 2). Thus, some shales and siltstones thus likely have some first cycle material. The high CIA's estimated for the unmetasomatised shales and siltstones associated with the wackes and the high percentage of quartz relative to other minerals in all sandstones suggests relatively intense weathering of any first cycle sediment.

5.4. Provenance composition—trace elements

As mentioned in the results section, elemental ratios that are critical in determining the composition of the provenance are significantly different between the shales and siltstones associated with the arenites and those associated with the wackes. The log of the (La/Lu)cn, La/Sc, Th/Sc, La/Co, and La/Cr ratios are significantly lower and the log of the Eu/Eu* are significantly higher in shales and siltstones associated with the wackes than those associated with the arenites using the Student *t*-test. The log of elemental ratios converts constant sum data (in which the sum of all analyzed elements must add to 100%) to a set of continuous variables that can range to infinity. Therefore, log-transformed data can be compared using parametric tests such as the Student *t*-test (Cardenas et al., 1996). This suggests that the shales and siltstones associated with the wackes may have received more input from an intermediate rock like granodiorite or tonalite, whereas, those associated with the arkoses received more input from more silicic rocks like granite. This is consistent with the higher percentage of plagioclase observed in the associated wackes than those in the arenites.

This possible input from granodiorite is illustrated in a La–Th–Sc diagram (Fig. 7). The shales and siltstones associated with the wackes extend more toward the hypothesized grandiorite–tonalite (intermediate) composition, but those associated with the arenites extend more toward the hypothesized granite composition. The composition of basalts are also plotted in Fig. 7. The composition of basalt does not quite fall in line with the extended range of composition of the shales and siltstone. This is consistent with the hypothesis that basalts did not contribute to the composition of the shales and siltstones. Thus, shales and siltstones derived from a provenance of granite and granodiorite–tonalite could have formed by intermediate mixing between these two extremes. Plots of various elemental ratios of shales and siltstones are also consistent with the range of their compositions being formed by mix-

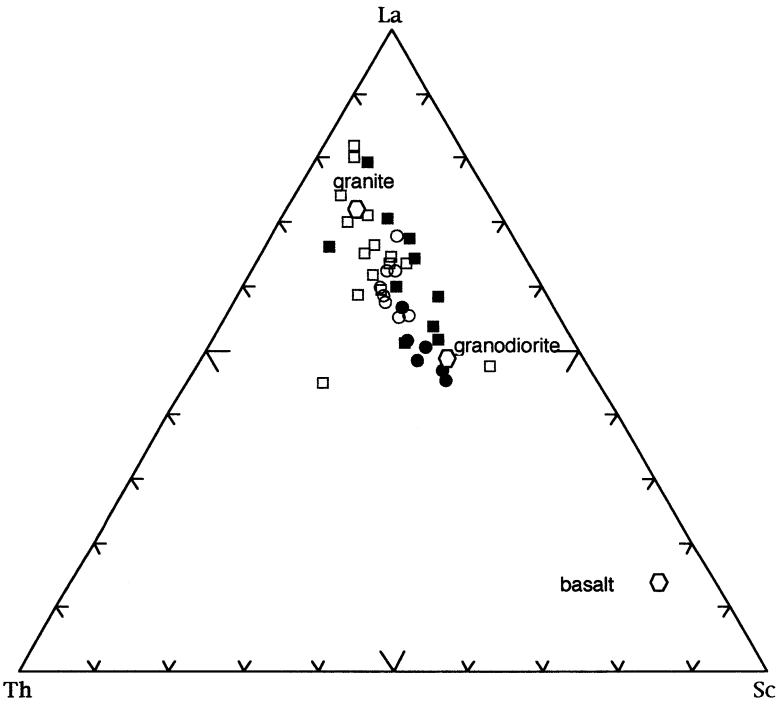

Fig. 7. The La–Th–Sc plot of the wackes, arenites, and associated shales and siltstones suggest variation due to composition of the source (same symbols as in previous diagrams). Most of the sandstone, shales and siltstones range between the composition of granite to granodiorite sources, suggesting that they formed by a mix of these two end-members. Basalts do not fall in line with the trend of the sedimentary rocks so they are not likely to be a source for the sedimentary rocks.

ing of granite and granodiorite end members, but not from basalt (e.g. Fig. 8). The Eu/Eu* and Th/Sc ratios of shales–siltstones plot along a linear trend. Unfortunately the composition of potential granites or granodiorites observed in this area have not been determined so hypothesised Eu/Eu* and Th/Sc ratios of these rocks were assumed. These assumed ratios are consistent with the composition of such rocks elsewhere. The range of compositions of the shales and siltstones could be formed by a mix of a granite source with an Eu/Eu* = 0.5 and Th/Sc = 1.18 and granodiorite–tonalite with an Eu/Eu* = 0.7 and Th/Sc = 0.5. Again, note that a basaltic source does not fall in line with the linear trend of the plotted shales and siltstones, thus, suggesting that basalts are not the significant source of the sedimentary rocks.

The above elemental ratios of the shales and siltstones associated with the sandstones are similar to the ratios of rocks derived from a silicic provenance like the shales of the near-by Lakhanda group or from the southwestern US (Table 5). The range of Eu/Eu* of most shales and siltstones associated with the arkoses are similar in composition to those of the recycled mudrocks likely derived from intermediate to silicic rocks in the southeastern USA (Table 5). The ranges of Eu/Eu* and Th/Sc ratios are similar to muds derived from some continental arc basins (samples CA-29M and CA30-M; McLennan et al., 1990). Many of the shales and siltstones of the Ui group have low ICV's, suggesting intense weathering of first cycle sediments or recycling may have occurred. The Eu/Eu* values of shales and siltstones associated with the wackes are higher than those of those associated with the arenites, and they also contain the highest ICV's, suggesting more first cycle input of more intermediate composition similar to mudrocks in the southeastern USA (Table 5).

Table 5
The range of elemental ratios of shales in this study are compared with those of fine fractions derived from silicic and basic source rocks

	Arenite shales–siltstone	Turbidite shales–siltstone	Arenite	Wackes	Range of fine fractions from silicic sources [a]	Range of fine fractions from basic sources [a]	Belaya river-near source [a]	Maya river-platform [b]
Eu/Eu*	0.51–0.64	0.55–0.71	0.46–0.80	0.61-0.78	0.32–0.83	0.70–1.02	0.35–0.66	0.36–0.67
La/Sc	2.2–4.0	1.3–2.4	1.2–20.8	1.7–11.5	0.70–27.7	0.40–1.1	1.75–3.39	1.92–2.75
Th/Sc	0.80–1.6	0.58–0.88	0.34–3.5	0.55–3.0	0.64–18.1	0.05–0.4	0.79–1.54	0.73–1.02
La/Co	1.0–6.7	0.80–3.0	1.1–54.7	1.4–8.2	1.4–22.4	–	7.11–11.3	7.37–12.0
Th/Co	0.41–2.1	0.32–1.3	0.5–9.3	0.41–2.6	0.30–7.5	–	0.44–4.77	0.52–5.86
Th/Cr	0.16–0.29	0.16–0.22	0.1–0.67	0.07–0.51	0.067–4.0	0.002–0.045	0.17–0.25	0.17–0.27

[a] From Cullers (2000).
[b] From Taylor and McLennan (1985).

The arenites are more variable in trace element ratios than the wackes due their large range in composition. Thus, the log of the elemental ratios between the wackes and arenites are not significantly different in most cases. Still the log of the Eu/Eu* of the arenites is significantly lower and the Th/Co and Th/Sc ratios of the arenites are significantly higher than the values obtained for the wackes. Sandstones are less likely to represent the Eu/Eu* and Th/Sc ratios in the source than are these ratios in shales and siltstones (Cullers, 1988, 1994a; Cullers et al., 1988). Thus, no quantitative modeling has been done on the variable composition of the sandstones as has been done for the shales and siltstones. The wackes, however, mostly plot closer to the hypothesized granodiorite–tonalite composition than do the arenites in the La–Th–Sc plots (Fig. 7). This relationship also suggests more input of granodiorite to tonalite into the wackes relative to the arenites. Of course, a source dominated by granite in the arenites is consistent with the abundant quartz and alkali feldspar observed in the petrography of the arenites. The abundant shale and siltstone fragments, quartz, and plagioclase > alkali feldspar observed in the wackes supports a granodiorite to tonalite source.

Thus, the trace element compositions of the arenites and wackes, and associated shales and siltstones are consistent with the origin suggested by major element and petrologic analyses. The A–CN–K diagrams and trace element compositions of wackes and associated shales and siltstones suggest that K-metasomatism changed the composition of these sedimentary rocks. The tonalitic source was most likely not Archean since such sources commonly exhibit high (La/Lu)cn and Eu/Eu* values. This interpretation is consistent with the Sm–Nd age of the shales and siltstones in the Ui Group that have

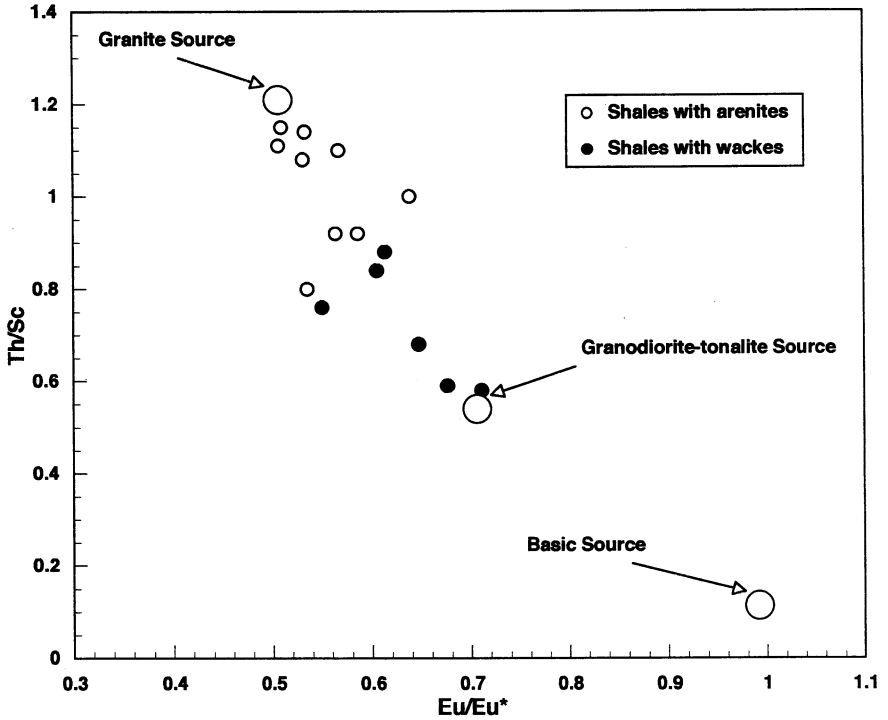

Fig. 8. A plot of Eu/Eu* and Th/Sc ratios of the shales and siltstones form a linear trend which plot between a hypothesized granite source and granodiorite (intermediate) source. Again basalt compositions do not fall in line with the trend of the shales and siltstones so basalts are not a likely source.

Mesoproterozoic model Nd ages ($T_{Nd}(DM) = 1.76–2.12$ Ga, $\varepsilon Nd(T) = -2.2$) that are pre-Riphean in age (Podkovyrov, in preparation). These ages are comparable with ages of the illitic shale in the Ignikan section that lies below the Lakhanda group ($T_{Nd}(DM) = 1.8–1.9$ Ga in the Gornostakh section and 1.55–1.66 Ga in the Maya plate samples) (Podkovyrov, in preparation). Kaolinite–montmorillonite–illite shale of the upper part of the Lakhanda group, however, have younger Nd model ages ($T_{Hd}(DM) = 1.39–1.51$ Ga, $\varepsilon Nd(T)$ up to $+2.2$) that likely reflects some input of mantle derived basic source rocks. In addition, the Proterozoic age of most of the zircons derived from Riphean sedimentary rocks in this area strongly supports a post-Archean source of the Ui group (Khudoley et al., 2001).

The arkosic sandstones of the Ui group contain mostly alkali feldspar, and trace element compositions of the arenites and associated shales and siltstones suggest a more silicic source than those of the wackes and associated shales and siltstones. The shales of the Lakhanda group contain major and trace element compositions similar to the shales and siltstones associated with the arenites of the Ui group, suggesting that they formed from a similar provenance. The high CIA's of the shales from the Lakhanda group also suggest that they formed by intense weathering just like those of the Ui group.

It has been hypothesized that the Ui group was deposited in an arm of a large rift system as part of the Rodinia supercontinent between 1030 and 1000 Ma (Khudoley et al., 2001). In addition, the sediment deposited in the Ui group has been hypothesized to have been derived from two sources (Khudoley et al., 2001). One source was from the Siberian craton to the west and the second was possibly from a non-Siberian-recycled orogen to the east and southeast. The current study is consistent with the two hypothesized sources.

6. Summary

1. The Ui group consists of quartz-rich arenite, wackes, and associated illite quartz shales and siltstones. The arenites contains generally more alkali feldspar than plagioclase. The wackes contain more plagioclase than alkali feldspar, and mostly shale–siltstone fragments. Thus, the arenites were likely derived from mostly a granite provenance, whereas, the wackes were likely derived from mostly a granodiorite–tonalite provenance.
2. Plots of wackes and associated shale and siltstone compositions in an A–CN–K diagram suggest that they were altered by K-metasomatism. Extrapolation of the composition of the shales and siltstones back to the alkali feldspar–plagioclase line suggests that the source of the fine-grained rocks were, like the associated wackes, derived from a source with more plagioclase than alkali feldspar. Plots of shale and siltstone compositions associated with the quartz-rich arenites in an A–CN–K diagram were scattered so that they could not be extrapolated back to the alkali feldspar–plagioclase line very well. Nevertheless, the range of the composition of the extrapolation appears to plot at higher alkali feldspar to plagioclase ratios than do the shales and siltstones associated with the wackes. Thus, this is consistent with the granite source determined petrographically for the arenites.
3. The high ICV's of some shales and siltstones suggest that they contain much first cycle material. Some shales–siltstones have lower ICV's that suggest they contain recycled sediment or that weathering of the first cycle material was intense. The high CIA's (81–85) estimated for the shales–siltstones prior to metasomatism suggest that intense weathering was probable.
4. Elemental ratios of these sedimentary rocks like (La/Lu)cn, Th/Sc, La/Sc, La/Co, La/Cr, and Eu/Eu* are consistent with their derivation from mostly granitoids as suggested by the petrography of the sandstones. These elemental ratios of the shales and siltstones plot in well-defined trends. For example, the Th/Sc ratios of shales and siltstones associated with the arenites are higher than those from the

wackes (1.2 vs. 0.51 maximum difference, respectively), and the Eu/Eu* of the shales and with the arenites are lower than those associated with the wackes (0.56 vs. 0.71). The shales–siltstones associated with the arenites and wackes could thus be derived from a mix of two end-member granitoids, one a granite and one a granodiorite–tonalite, with a similar range of Eu/Eu* and Th/Sc ratios as those of the shales and siltstones. Plots of elemental ratios of the wackes and arenites are quite scattered so no quantitative modeling was done on them.

Acknowledgements

We thank the crew of the Kansas State University reactor for irradiating our samples and to the Department of Mechanical-Nuclear Engineering for the use of their detector–analyzer system for neutron activation analyses. We also thank C. Fedo, M. Bhatia and Gary Girty for constructive reviews.

References

Allegre, C.J., Rousseau, D., 1984. The growth of the continent through time studied by Nd isotope analyses of shales. Earth Planet. Sci. Lett. 67, 19–34.

Barshad, I., 1966. The effect of a variation in precipitation on the nature of clay mineral formation in soils from acid and basic igneous rocks. Proc. Int. Clay Conf., 167–173.

Bavinton, O.A., Taylor, S.R., 1980. Rare-earth element geochemistry of Archean metasedimentary rocks from Kambalda, Western Australia. Geochim. Cosmochim. Acta 44, 639–648.

Bhatia, M.R., 1983. Plate tectonics and geochemical composition of sandstones. J. Geol. 91, 611–627.

Bhatia, M.R., 1985. Rare earth element geochemistry of Australian Paleozoic graywackes and mudrocks: provenance and tectonic control. Sediment. Geol. 45, 97–113.

Bhatia, M.R., Crook, K.A.W., 1986. Trace element characteristics of graywackes and tectonic setting discrimination of sedimentary basins. Contrib. Mineral. Petrol. 92, 181–193.

Cardenas, A.A., et al., 1996. Assessing differences in composition between low metamorphic grade mudstones and high-grade schists using log ratio techniques. J. Geol. 104, 279–293.

Condie, K.C., Wronkiewicz, D.J., 1990. The Cr/Th ratio in Precambrian pelites from the Kaapvaal craton as an index of craton evolution. Earth Planet. Sci. Lett. 97, 256–267.

Cox, R., Low, D.R., Cullers, R.L., 1995. The influence of sediment recycling and basement composition on evolution of mudrock chemistry in the southwestern United States. Geochim. Cosmochim. Acta 59, 2919–2940.

Cullers, R.L., 1988. Mineralogical and chemical changes of soil and stream sediment formed by intense weathering of the Danberg granite, Georgia, USA. Lithos 21, 301–314.

Cullers, R.L., 1994a. The chemical signature of source rocks in size fractions of Holocene stream sediment derived from metamorphic rocks in the Wet Mountains region USA. Chem. Geol. 113, 327–343.

Cullers, R.L., 1994b. The controls on the major and trace element variation of shales, siltstones, and sandstones of Pennsylvanian–Permian age from uplifted continental blocks in Colorado to platform sediment in Kansas, USA. Geochim. Cosmochim. Acta 58, 4955–4972.

Cullers, R.L., 1995. The controls on the major- and trace-element evolution of shales, siltstones, and sandstones of Ordovician to Tertiary age in the Wet Mountains region, Colorado, USA. Chem. Geol. 123, 107–131.

Cullers, R.L., 2000. The geochemistry of shales, siltstones, and sandstones of Pennsylvanian–Permian age, Colorado, USA: implications for provenance and metamorphic studies. Lithos 51, 181–203.

Cullers, R.L., Berendsen, P., 1998. The provenance and chemical variation of sandstones associated with the mid-continent rift system, USA. Eur. J. Mineral. 10, 987–1002.

Cullers, R.L., Podkovyrov, V.M., 2000. Geochemistry of the mesoproterozoic Lakhanda shales in southeastern Yakutia, Russia: implications for mineralogical and provenance control, and recycling. Precambrian Res. 104, 77–93.

Cullers, R.L., Ramakrishnan, S., Berendsen, P., Griffin, T., 1985. Geochemistry and petrogenesis of lamproites, late cretaceous age, Woodson Co, Kansas, USA. Geochim. Cosmochim. Acta 49, 1383–1402.

Cullers, R.L., Barrett, T., Carlson, R., Robinson, B., 1987. Rare-earth element and mineralogic changes in Holocene soil and stream sediment: a case study in the Wet Mountains, Colorado, USA. Chem. Geol. 63, 275–297.

Cullers, R.L., Basu, A., Suttner, L., 1988. Geochemical signature of provenance in sand-size material in soils and stream sediments near the Tobacco Root batholith, Montana, USA. Chem. Geol. 70, 335–348.

Dickinson, W.R.T., 1985. Interpreting provenance relations from detrital modes of sandstones. In: Zuffa, G.G. (Ed.), Provenance of Arenites. NATO ASI, pp. 333–361 series C.

Dickinson, W.R., Suczek, C.A., 1979. Plate tectonics and sandstone compositions. Am. Assoc. Petrol. Geologists 63, 2164–2182.

Fedo, C.M., Nesbitt, H.W., Young, G.M., 1995. Unraveling the effects of potassium metasomatism in sedimentary rocks and paleosols, with implications for paleoweathering conditions and provenance. Geology 23, 921–924.

Fedo, C.M., Young, G.M., Nesbitt, H.W., 1997a. Paleoclimatic control on the composition of the Paleoproterozoic Serpent Formation, Huronian Supergroup, Canada; a greenhouse to icehouse transition. Precambrian Res. 86, 201–223.

Fedo, C.M., Young, G.M., Nesbitt, H.W., Hanchar, J.M., 1997b. Potassic and sodic metasomatism in the southern province of the Canadian shield: evidence from the Paleoproterozoic Serpent Formation, Huronian Supergroup, Canada. Precambrian Res. 84, 17–36.

Gordon, G.E., et al., 1968. Instrumental neutron activation analysis of standard rocks with high resolution gamma-ray detectors. Geochim. Cosmochim. Acta 32, 369–396.

Ingersoll, R.V., et al., 1984. The effect of grain size on detrital modes: a test of the Gazzi-Dickinson point-counting method. J. Sediment. Petrology 54, 103–116.

Jacobs, J.W., Korotov, R.L., Blanchard, D.P., Haskin, L.A., 1977. A well-tested procedure for instrumental neutron activation analysis of silicate rocks and minerals. J. Radioanal. Chem. 40, 93–114.

Johnsson, M.J., 1988. First-cycle quartz arenites in the Orinoco river basin, Venezuela and Colombia. J. Geol. 96, 263–277.

Johnsson, M.J., 1993. The system controlling the composition of clastic sediments. In: Johnsson, M.J., Basu, A. (Eds.), Processes Controlling the Composition of Clastic Sediments. Geololgical Society of American Special Paper, pp. 1–19.

Johnsson, M.J., 2000. Tectonic assembly of east-central Alaska: evidence from Cretaceous–Tertiary sandstones of the Kandik River terrane. Geol. Soc. Am. Bull. 112, 1023–1042.

Khudoley, A.K., Rainbird, R.H., Stern, R.A., Kropachev, A.P., Heaman, L.M., Zanin, A.M., Podkovyrov, V.N., Bolova, V.N., Sukhorukov, V.I., 2001. Sedimentary evolution of the Riphean–Vendian basin of southeastern Siberia. Precambrian Res. 111, 129–163.

McLennan, S.M., Taylor, S.R., Eriksson, K.A., 1983. Geochemistry of archean shales from the Pilbara Supergroup, Western Australia. Geochim. Cosmochim. Acta 47, 1211–1222.

McLennan, S.M., Taylor, S.R., McCulloch, M.T., Maynard, J.B., 1990. Geochemistry and Nd–Sr isotopic composition of deep-sea turbidites, crustal evolution and plate tectonic associations. Geochim. Cosmochim. Acta 54, 2014–2050.

McLennan, S.M., Hemming, S., McDaniel, D.K., Hanson, G.N., 1993. Geochemical approaches to sedimentation, provenance, and tectonics. In: Johnson, M.J., Basu, A. (Eds.), Processes Controlling the Composition of Clastic Sediments. Geological Society of America, Colorado, Boulder, pp. 21–40.

Mongelli, G., Cullers, R.L., Muelheisen, S., 1996. Geochemistry of Late Cretaceous–Oligocene shales from the Varicolori Formation, southern Apennienes, Italy: implications for mineralogical, grain-size control and provenance. Eur. J. Mineral. 8, 733–754.

Nakamura, N., 1974. Determination of REE, Ba, Fe, Mg, Na and K in carbonaceous and ordinary chondrites. Geochim. Cosmochim. Acta 38, 757–775.

Nesbitt, H.W., Young, G.M., 1982. Early Proterozoic climates and plate motions inferred from major elemental chemistry of lutites. Nature 199, 715–717.

Nesbitt, H.W., Fedo, C.M., Young, G.M., 1996. Quartz and feldspar stability, steady and non-steady-state weathering, and petrogenesis of siliciclastic sands and muds. J. Geol. 105, 173–191.

Pavlov, V.E, Burakov, K.S., Tselmovich, V.A., Zhuravlev, D.Z., 1992. Paleomagnetics of sills from the Uchur-Maya region and estimation of geomagnetic field intensity in the late Riphean. Phys. Earth N1, 92–101.

Pettijohn, F.J., Potter, P.E., Siever, R., 1987. Sand and Sandstone. Springer, New York.

Pokrovsky, E.G., Vinogradov, V.I., 2001. Isotopic composition of oxygen in Riphean argillites of the Yudoma-Maya depression in connection with isotopic dating. Lithol. Miner. Res. 6, 646–653 in Russian.

Rainberd, R.H., et al., 1998. U–Pb geochronology of Riphean sandstone and gabbro from southeast Siberia and its bearing on the Laurentia–Siberia connection. Earth Planet. Sci. Lett. 164, 409–420.

Roser, B.P., Korsch, R.J., 1986. Determination of tectonic setting of sandstone–mudstone suites using SiO_2 content and K_2O/Na_2O ratio. J. Geol. 94, 635–650.

Roser, B.P., Korsch, R.J., 1988. Provenance signatures of sandstone–mudstone suites determined using discriminant function analysis of major-element data. Chem. Geol. 67, 119–139.

Semikhatov, M.A., 1991. General problems of Proterozoic stratigraphy in the USSR, Soviet Science Review Geology, vol. 1. Harwood Academic Publishers, New York, p. 192.

Semikhatov, M.A., Serebrykov, S.N., 1983. The Siberian Hypostratotype of the Riphean. Nauka Press, Moskow, p. 224.

Sukhorukov, V.I., 1986. The upper Riphean type sections of the Ulakhan–Bam ridge. In: Khomentovsky, V.V. (Ed.), Late Precambrian and early Paleozoic of Siberia: Siberian Platform and outer part of the Altai–Sayan fold belt. IGG Press, Novosibirsk, pp. 23–64.

Taylor, S.R., McLennan, S., 1985. The Continental Crust; its composition and evolution. Blackwell Press, Oxford, 312 pp.

Taylor, S.R., McLennan, S.M., 1991. Sedimentary rocks and crustal evolution; tectonic setting and secular trends. J. Geol. 99, 1–21.

Van de Kamp, P.C., Leake, B.E., 1985. Petrography and geochemistry of feldspathic and mafic sediments of the northeastern Pacific margin. Trans. R. Soc. Edinburgh Earth Sci. 76, 411–449.

Vinogradov, B.G., et al., 1998. Isotopic evidences of epigenetic transformations and the problem of the age of Riphean rocks in the Uchar–Maya region eastern Siberia. Lithol. Miner. Resour. 33, 561–576 Translated from Litologiya i Poleznye Isfcopaemye.

Wronkiewicz, D.J., Condie, K.C., 1990. Geochemistry and mineralogy of sediments from the Ventersdorp and Transvaal supergroups, South Africa: cratonic evolution during the early Proterozoic. Geochim. Cosmochim. Acta 54, 343–354.